High-Frequency Electrodynamics of $Bi_2Sr_2CaCu_2O_{8+\delta}$: Nonlinear Response in the Vortex State

R. Mallozzi and J. Orenstein

Materials Sciences Division, Lawrence Berkeley National Laboratory and Physics Department, University of California, Berkeley, California 94720

J. N. Eckstein and I. Bozovic

E. L. Ginzton Research Center, Varian Associates, Inc., Palo Alto, California 94304-1025

(Received 10 January 1997)

Coherent terahertz spectroscopy is used to measure the complex conductivity of thin films of $Bi_2Sr_2CaCu_2O_{8+\delta}$ in the vortex state as a function of frequency, temperature, and applied magnetic field. We report an unusual sublinear power law dependence of the high-frequency magnetoconductivity $\Delta\sigma(H) \equiv \sigma(H) - \sigma(0)$ on magnetic field. Over a broad range of field and temperature, $\Delta\sigma_2$ varies as H^α, with $\alpha \approx \frac{1}{2}$. We present a model based on the nonlinear London electrodynamics predicted for a d-wave superconductor which quantitatively explains these results using only parameters obtained from zero-field measurements. [S0031-9007(98)06220-6]

PACS numbers: 74.25.Gz, 74.25.Nf, 74.60.–w, 74.76.Bz

There is widespread agreement that the high-T_c cuprates are "unconventional" superconductors whose properties are at odds with expectations based on s-wave pairing. However, the impact of unconventional gap structure on some of their macroscopic properties has not been fully appreciated. For example, the high-frequency electrodynamics of the vortex state have been widely assumed to reflect the dynamics of vortex motion as in conventional superconductors. In this paper we report measurements in the high-T_c superconductor $Bi_2Sr_2CaCu_2O_{8+\delta}$ (BSCCO) which are not consistent with this assumption. We describe an alternative picture based on the nonlinear London relation in unconventional superconductors [1–3]. We show that this picture accounts quantitatively for vortex-state electrodynamics, without reference to phenomenological pinning force constants or viscosities, using only parameters obtained from zero-field measurements. Within this model, the vortex-state electrodynamic response provides a high-resolution spectrum of the quasiparticle density of states in the superconducting state.

High-frequency measurements provide a direct test of models of vortex-state electrodynamics [4]. The response is probed using low currents (10^{-5} of the critical current) at frequencies where pinning is unimportant. We use time-domain spectroscopy to continuously span the frequency ($\omega/2\pi$) range from 50 to 250 GHz. We focus on the change in the response functions, $\sigma(\omega)$ or $\rho(\omega)$, due to the application of static magnetic fields above the first critical field H_{c1}. Using coherent detection to determine both amplitude and phase of the transmission coefficient, we can directly determine the complex response functions without assumptions or additional measurements.

The samples are 655 and 740 Å thick BSCCO films grown on [100] $LaAlO_3$ using atomic layer-by-layer molecular beam epitaxy, with resistively measured T_c's of 78–80 K. The films are c-axis oriented so that the high-frequency E field lies in the a-b plane. The composition of the samples is carefully controlled to ensure that they are free of second-phase defects [5]. Their resistance R is linear in T above T_c. The ratio $R(300\ \mathrm{K})/R(0)$ is ≈ 10, where $R(0)$ is the extrapolated resistance at $T = 0$. Recent high-resolution photoemission on films grown under the same conditions show normal and superconducting spectra consistent with the bulk-crystal analog [6].

Figure 1 presents the H and T dependences of $\Delta\sigma$ measured near the center of our frequency range, at $\omega/2\pi = 150$ GHz, for H along the c axis. Panels (a) and (b) show the real and imaginary parts of $\Delta\sigma$, respectively, as a function of magnetic field up to 7 T,

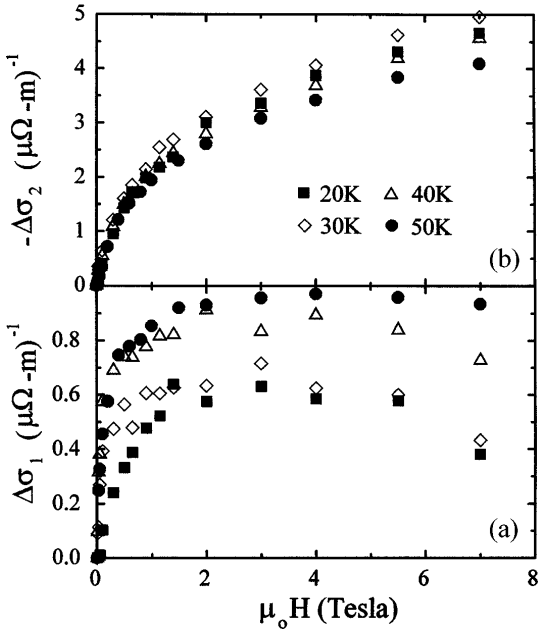

FIG. 1. Real and imaginary parts of $\Delta\sigma \equiv \sigma(H) - \sigma(0)$ at 150 GHz.

for several temperatures. The change in conductivity with field is highly nonlinear, despite the fact that the average vortex density is linearly proportional to H. The imaginary part, σ_2, drops with increasing field to about 60% of its zero-field value. $|\Delta\sigma_2|$ varies approximately as H^α (with $\alpha \approx \frac{1}{2}$) and is remarkably insensitive to T given the large changes in vortex mobility over the measured range. The changes in the real part of the conductivity, σ_1, are more complex. At low H, σ_1 increases in parallel with the decrease in σ_2. At larger H, σ_1 flattens and eventually decreases.

Models based on vortex motion [7–10] have been used almost universally to account for changes in electrodynamic response due to magnetic fields above H_{c1}. For example, an increase in surface resistance, R_s (at 45 GHz), proportional to $H^{1/2}$ for fields above 0.1 T was recently reported in $Bi_2Sr_2CaCu_2O_{8+\delta}$ single crystals [11]. This dependence on H was ascribed to free flow of vortices, where $\Delta R_s \propto H^{1/2}$ obtains at high fields [12]. Because interpretations based on vortex motion are so widely assumed, we begin by comparing our results with the predictions of vortex dynamics models.

While the $\Delta\sigma(\omega)$ shown in Fig. 1 is consistent with $\Delta R_s \propto H^{1/2}$, resolving both real and imaginary components of the response shows that the electrodynamics cannot be explained by free-flux flow. The free-flow conductivity is simply the reciprocal of the Bardeen-Stephen resistivity $\rho_{B\text{-}S}$, implying a $\Delta\sigma$ that is real and proportional to $1/H$. Our data show instead that $\Delta\sigma$ is predominantly imaginary and proportional to $H^{1/2}$. $\Delta\sigma_2$ dominates the behavior of the R_s, leading to $\Delta R_s \propto H^{1/2}$.

While the observation that $\Delta\sigma_2 > \Delta\sigma_1$ is inconsistent with free-flux flow, it does not rule out all models based on vortex motion. Changes in the imaginary part of σ appear in vortex dynamic models that go beyond free flow of vortices and include pinning [7–10]. These models enable calculation of the vortex-induced resistivity $\Delta\rho(H)$ from *dc* to high frequencies in terms of phenomenological viscosity, pinning, and disorder parameters.

For comparison of vortex models to our data we use the work of Coffey and Clem (CC) [8], which neatly exhibits the essential aspects of the vortex dynamics picture. They modeled the vortex liquid as a Brownian particle diffusing on a periodic potential with amplitude U and curvature κ.

Figure 2 compares $\Delta\rho_1$ obtained from the model (solid lines) with $\Delta\rho_1$ measured at *dc* (circles) [13] and at high frequency (squares). The resistivity has been normalized to the Bardeen-Stephen resistivity to provide a useful dimensionless measure of the magnetoresistivity per vortex.

Departures from linear $\Delta\rho(H)$ arise in the model when the barrier height U is field dependent. Adjusting this parameter for best fit allows the model to account well for the *dc* data, but the $U(H)$ obtained fails to describe, even qualitatively, the high-frequency data. The magnetoresistivity per vortex becomes singular at low H, while the CC resistivity becomes field independent. To describe the high-frequency data, $U(H)$ would have to have the opposite field dependence at high frequency as it does at low. This artificial requirement contrasts with the natural explanation that follows from d-wave electrodynamics.

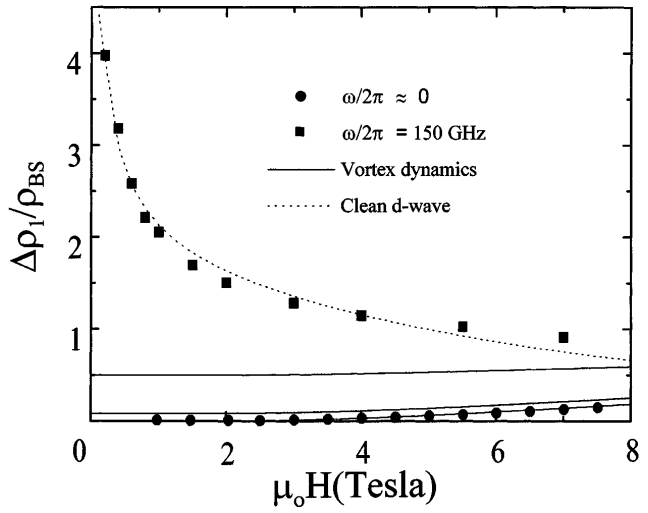

FIG. 2. Re$[\Delta\rho]$ normalized to the Bardeen-Stephen resistivity provides a dimensionless measure of the dissipation per vortex. Representative data at $\omega/2\pi = 150$ GHz, $T = 50$ K, (solid squares) show a dramatic divergence as $H \to 0$. This behavior is not present in a model based on vortex dynamics, shown as solid lines for $\omega\tau_0 = 0$, 3, and 1 (the curves approach a flat line at unity as $\omega\tau_0 \to \infty$). τ_0 is the characteristic vortex relaxation time in the model. The dashed line through the 150 GHz data is a fit to the model discussed in the text, based on d-wave superconductivity.

This alternative model is based on the intrinsic nonlinear response of superconductors [14], as it is manifested in d-wave materials [1–3]. The London relation $\vec{J}_s = n_s e(\vec{v}_s)\vec{v}_s$ expresses the electrodynamic response of the superfluid. [Here n_s is the superfluid density and $m^*\vec{v}_s = \nabla\varphi/2 + (2e/c)\vec{A}$, where m^* is the Cooper pair mass and φ is the condensate phase.] The London relation is nonlinear because the creation energy of a quasiparticle of velocity $\vec{v}$ shifts by $\varepsilon_{qp}(\vec{v}) = (m^*/2)\vec{v}_s \cdot \vec{v}$ in the presence of a superflow [15]. The decrease in creation energy for quasiparticles whose velocity opposes the superflow leads to enhanced quasiparticle occupation and reduced n_s. In s-wave superconductors the reduction in n_s is exponentially small until ε_{qp} approaches Δ. For d-wave superconductors with maximum gap Δ_0, Yip and Sauls [1,2] predicted a much larger change in n_s because quasiparticle creation energies extend down to zero. They found a fractional reduction given by $-\Delta n_s/n_s \approx 2\varepsilon_{qp}/\mu\Delta_0$, where $\mu\Delta_0$ is the rate of increase of the gap with angular displacement from the node, $\partial\Delta(\theta)/\partial\theta$.

The vortex state is accompanied by a strong and inhomogeneous superflow field. The range of ε_{qp} associated with this flow extends up to Δ_0. In the following we determine if the resulting depletion in superfluid density can account for vortex-state electrodynamics in BSCCO.

As a first step, we quantify the change in $\sigma(\omega)$ due to a reduction in n_s. Our starting point is the two-fluid model,

which describes the conductivity in the superconducting state as the sum of normal and superfluid contributions, i.e., $\sigma = \sigma_s + \sigma_n$, where $\sigma_s = in_s e^2/m^*\omega$ and $\sigma_n = n_n e^2/m^* S(\omega)$. $S(\omega)$ is the frequency dependence of the quasiparticle conductivity. The cuprates are clean limit superconductors in which $n_s + n_n$ equals the normal state carrier density n. The change in σ due to a conversion of super to normal fluid [assuming $S(\omega)$ is unchanged] is proportional to $\Delta x_n \equiv \Delta n_n/n$. It is given by

$$\Delta\sigma = \omega_p^2 \Delta x_n [S(\omega) - i/\omega], \qquad (1)$$

where ω_p is the plasma frequency. Equation (1) predicts a reduction σ_2 proportional to Δx_n for frequencies below the quasiparticle scattering rate (where S is purely real).

Because the superflow in the vortex state is spatially nonuniform, we must average the local change $\Delta x_n(r)$ over the unit cell of the vortex lattice. We approximate the Wigner-Seitz cell as a circle of radius $R/2$, where $R = 2(\varphi_0/\pi H)^{1/2}$ is the intervortex separation, to obtain

$$\Delta\overline{x}_n(R) \cong \frac{1}{\pi(R/2)^2} \int^{R/2} 2\pi r \Delta x_n(r)\, dr\,, \qquad (2)$$

where $\Delta\overline{x}_n$ is the spatial average of $\Delta x_n(r)$. Notice that $\Delta\overline{x}_n$ has acquired an implicit dependence on H through the upper limit of integration $R/2$.

The form of $\Delta\overline{x}_n(H)$ expected for a clean d-wave superconductor can be easily derived by analogy to the calculation of the density of states in the vortex state [16]. The Yip-Sauls prediction for $\Delta x_n(\varepsilon_{\rm qp})$, together with the vortex superflow relation $v_s(r) = \hbar/m^* r$, predicts a local increase in normal density proportional to $1/r$. Substituting $\Delta x_n(r) \propto 1/r$ into Eq. (2) yields $\Delta\overline{x}_n \propto 1/R \propto H^{1/2}$. Thus d-wave superconductivity provides a natural explanation for power law variation in the magnitude of the electrodynamic response functions, which is closely related to power laws seen in the specific heat [17].

While the variation of $\Delta\sigma_2$ with H shown in Fig. 1 is close to the predicted power law of $\frac{1}{2}$, it is measurably different. To describe the departure from the clean d-wave prediction, we no longer assume the Yip-Sauls result $\Delta x_n \propto \varepsilon_{\rm qp}$ as in the previous analysis. Instead, we determine Δx_n as a function of either $\varepsilon_{\rm qp}$ or r directly from the experimental data, using the procedure described below.

Using Eq. (1), we obtain $\Delta\overline{x}_n(H)$ from the measured $\Delta\sigma_2(\omega)$. This function determines $\Delta x_n(r)$, as can be seen by differentiating both sides of Eq. (2) with respect to R,

$$\Delta x_n(r) = \frac{1}{4r}\frac{d}{dR}\left[R^2 \Delta\overline{x}_n(R)\right]|_{R/2=r}\,. \qquad (3)$$

In Fig. 3 we plot Δx_n obtained from Eq. (3) as a function of $1/r$, rather than r, for reasons which we clarify momentarily. Our experiment accesses a range of r from 100–1200 Å, or half the vortex separation in the field range from 0.05 to 7 T. The $\Delta x_n(1/r)$ shown in Fig. 3 is very different from that expected for vortices in an s-wave superconductor with the same average gap. For the s-wave case we expect Δx_n to be unity within approximately 15 Å of the vortex center and fall to essentially zero outside this "core."

The plot of $\Delta x_n(1/r)$ depicts $\Delta x_n(\varepsilon_{\rm qp})$ as well because the scale of $1/r$ is linearly proportional to $\varepsilon_{\rm qp}$. Given that $v_s = \hbar/m^* r$, the local $\varepsilon_{\rm qp}$ is simply $\hbar v_{nF}/2r$ when the current is along a nodal direction. ($\vec{v}_{nF}$ is the Fermi velocity near the node.) Since the vortex current is circular, we must average over all directions of superflow. This introduces a factor of $4/\pi$ and gives an average quasiparticle energy shift $\langle\varepsilon_{\rm qp}\rangle$ at distance r from the vortex center of $(2/\pi)(\hbar v_{nF}/r)$. To convert the $1/r$ to a scale of $\langle\varepsilon_{\rm qp}\rangle$ we use $\hbar v_{nF} = 140$ meV nm, the value determined from angle-resolved photoemission (ARPES) in the normal state [18].

Performing this conversion in Fig. 3, we see that Δx_n vs $\langle\varepsilon_{\rm qp}\rangle$ is linear for quasiparticle energies greater than $\approx$3 meV. Recall that the clean d-wave model indeed predicts that Δx_n vs $\langle\varepsilon_{\rm qp}\rangle$ is linear, with the same constant of proportionality that relates θ to $\Delta(\theta)$ near the node. The dashed line through the data points in Fig. 3 is not a fit, rather it is a plot of θ vs $\Delta(\theta)$ taken directly from ARPES in the superconducting state [19]. The remarkable agreement in slope, $(54\ \text{meV})^{-1}$, between these two experiments indicates that d-wave nonlinearity quantitatively describes vortex-state electrodynamics in BSCCO. This description involves no adjustable parameters, only independently measured zero-field parameters: ω_p, $\hbar v_{nF}$, and $\mu\Delta_0$.

Figure 3 shows that $\Delta x_n(\varepsilon_{\rm qp})$ is nonlinear at low energies. The departure from linearity below $\approx$3 meV corresponds to a departure from $H^{1/2}$ behavior for fields below 0.2 T. Possible origins for this departure are nonzero temperature, disorder, and probing frequency. The fact that the departure from linearity remains at 3 meV over a broad range of temperature up to 60 K tends to rule

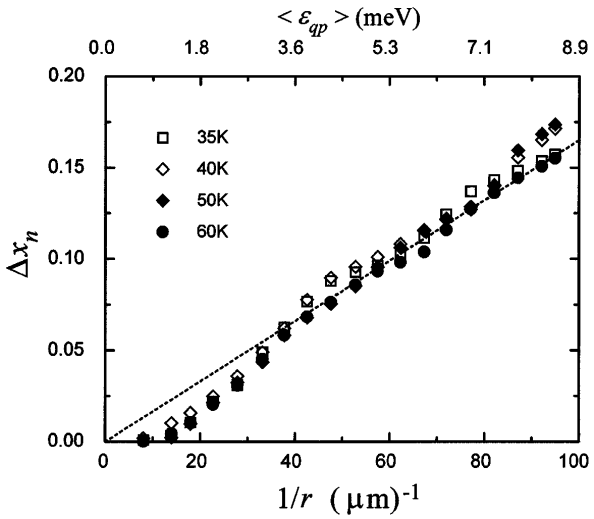

FIG. 3. Change in the fraction of normal electrons Δx_n vs inverse distance from the vortex core $1/r$ (lower axis) and vs quasiparticle energy shift $\langle\varepsilon_{\rm qp}\rangle$ (upper axis). The dashed line shows the rate of gap increase away from the node as determined by angle-resolved photoemission.

out finite temperature effects. Another possibility is a deviation from the clean d-wave density of states near 3 meV above the Fermi energy. Finally, it is possible that the departure from linearity is related to the probing frequency [20]. At each point in the sample, the superflow modifies the quasiparticle density of states (QPDOS) only at energies below the local value of ε_{qp}. Consequently, we expect $\Delta\sigma$ to become smaller when probe photon energy $\hbar\omega$ begins to exceed ε_{qp}. Our measurements indicate that the departure from $H^{1/2}$ is indeed more pronounced at the high frequency end of our range [21].

The above discussion demonstrates that d-wave nonlinearity accounts well for the reduction in superfluid density, and consequently in σ_2, due to magnetic fields. This effect alone is clearly not sufficient to account for the more complex changes in σ_1 shown in Fig. 1. From Eq. (1) we expect that $\Delta\sigma_1$ may be more complicated than $\Delta\sigma_2$, because $S(\omega)$ can change with applied field, due to a field-dependent quasiparticle scattering rate, for example, [22]. The small jump in σ_1 at very small fields could be due to extrinsic effects.

The success of d-wave nonlinearity in explaining high-frequency electrodynamics in BSCCO suggests a reexamination of the most heavily studied cuprate superconductor, $YBa_2Cu_3O_7$ (YBCO). YBCO differs from BSCCO in that $\Delta\sigma_2$ is nearly linear in field, as compared with $H^{1/2}$ [4,21]. Because of this linearity, vortex dynamic models with a field-independent κ seem to present a natural interpretation of the microwave magnetoconductivity. However, the vortex dynamics interpretation yields a characteristic relaxation rate in the tens of GHz regime [4], and predicts that above this frequency the changes in either σ or ρ will be purely real. Recently, Parks *et al.* [23] reported that $\Delta\sigma_2/\sigma_2$ remains the same up to frequencies as high as 500 GHz. Although they suggested the nonlinear London response as an alternate mechanism, the linearity of $\Delta\sigma_2$ with H presented a serious problem for this interpretation.

Given our observation of $H^{1/2}$ behavior in BSCCO, the issue of vortex-state electrodynamics in YBCO becomes more sharply defined. As the low-energy QPDOS is thought to be similar in both materials, d-wave nonlinearity should be seen in YBCO as well. The fact that the fractional reduction in n_s is *smaller* in YBCO [21] must be considered as well. One cannot argue, for example, that the vortex dynamic contribution in YBCO dominates the $H^{1/2}$ contribution, because then the total change must be greater.

We suggest instead that the magnetoconductivity in YBCO is dominated by essentially the same physics as in BSCCO. To explain linearity in H, the extent of normal fluid around each vortex must be cut off at about 10 nm, such as by a field-induced gap in the QPDOS. Another possible explanation is that spatial distribution of vortices in YBCO is inhomogeneous, as suggested by recent scanning tunneling microscopy observations of the mixed state [24]. If the intervortex separation does not vary simply as $H^{1/2}$, the $H^{1/2}$ singularity can be lost. Indeed, the small deviations from $H^{1/2}$ in BSCCO could reflect deviations from the equilibrium vortex spacing at low field, rather than an intrinsic effect.

To summarize, we have measured $\Delta\sigma(\omega, H, T)$ in BSCCO thin films. We found a power law dependence in H that is inconsistent with vortex motion. We explained these changes quantitatively using parameters available from zero-field measurements of the complex conductivity and ARPES, without introducing phenomenological vortex dynamic parameters. The success of this model suggests that the high-frequency electrodynamic response in the mixed state is dominated by enhanced pair breaking due to nodes in the gap function.

We acknowledge useful discussions with J. A. Sauls and D. J. Scalapino. This work was supported under NSF Grant No. FD95-10353, DOE Contract No. DE-AC03-76SF00098, and ONR Contract No. N00014-94-C-0011.

[1] S. K. Yip and J. A. Sauls, Phys. Rev. Lett. **69**, 2264 (1992).
[2] D. Xu, S. K. Yip, and J. A. Sauls, Phys. Rev. B **51**, 16 233 (1995).
[3] B. P. Stojkovic and O. T. Valls, Phys. Rev. B **51**, 6049 (1995).
[4] M. Golosovsky, M. Tsindlekht, and D. Davidov, Supercond. Sci. Technol. **9**, 1 (1996).
[5] J. N. Eckstein and I. Bozovic, Annu. Rev. Mater. Sci. **25**, 679 (1995).
[6] D. S. Marshall *et al.*, Phys. Rev. B **52**, 12 548 (1995).
[7] J. I. Gittleman and B. Rosenblum, Phys. Rev. Lett. **16**, 734 (1966).
[8] M. W. Coffey and J. R. Clem, Phys. Rev. Lett. **67**, 386 (1991).
[9] C. J. van der Beek, V. B. Geshkenbein, and V. M. Vinokur, Phys. Rev. B **48**, 3393 (1993).
[10] P. Martinoli *et al.*, Physica (Amsterdam) **165B & 166B**, 1163 (1990).
[11] Y. Matsuda *et al.*, Phys. Rev. Lett. **75**, 4512 (1995).
[12] Y. Matsuda *et al.*, Phys. Rev. B **49**, 4380 (1994).
[13] J. T. Kucera *et al.*, Phys. Rev. B **46**, 11 004 (1992). The low-frequency data shown are from this work, performed on similar films.
[14] S. Sridhar and J. E. Mercereau, Phys. Rev. B **34**, 203 (1986), and references therein.
[15] J. Bardeen, Phys. Rev. Lett. **1**, 399 (1958).
[16] G. E. Volovik, JETP Lett. **58**, 469 (1993).
[17] K. A. Moler *et al.*, Phys. Rev. Lett. **73**, 2744 (1994).
[18] D. S. Dessau, Phys. Rev. Lett. **71**, 2781 (1993).
[19] H. Ding *et al.*, Phys. Rev. B **54**, R9678 (1996).
[20] J. A. Sauls (private communication).
[21] J. Orenstein *et al.*, in The Superconducting State in Magnetic Fields: Special Topics and New Trends, edited by Carlos Sa de Melo (World Scientific, Singapore, to be published).
[22] K. Krishana *et al.*, Science **277**, 83 (1997).
[23] B. Parks *et al.*, Phys. Rev. Lett. **74**, 3265 (1995).
[24] O. Fischer *et al.*, Physica (Amsterdam) **282C–287C**, 315 (1997).